

Dynamic Buffers: Cost-Efficient Planning for Tabletop Rearrangement with Stacking

Arman Barghi, Hamed Hosseini, Seraj Ghasemi,
Mehdi Tale Masouleh, Ahmad Kalhor

Abstract—Rearranging objects in cluttered tabletop environments remains a long-standing challenge in robotics. Classical planners often generate inefficient, high-cost plans by shuffling objects individually and using fixed *buffers*—temporary spaces such as empty table regions or static stacks—to resolve conflicts. When only free table locations are used as buffers, dense scenes become inefficient, since placing an object can restrict others from reaching their goals and complicate planning. Allowing stacking provides extra buffer capacity, but conventional stacking is static: once an object supports another, the base cannot be moved, which limits efficiency. To overcome these issues, a novel planning primitive called the *Dynamic Buffer* is introduced. Inspired by human grouping strategies, it enables robots to form temporary, movable stacks that can be transported as a unit. This improves both feasibility and efficiency in dense layouts, and it also reduces travel in large-scale settings where space is abundant. Compared with a state-of-the-art rearrangement planner, the approach reduces manipulator travel cost by 11.89% in dense scenarios with a stationary robot and by 5.69% in large, low-density settings with a mobile manipulator. Practicality is validated through experiments on a Delta parallel robot with a two-finger gripper. These findings establish dynamic buffering as a key primitive for cost-efficient and robust rearrangement planning.

Index Terms—Rearrangement Planning, Dynamic Buffer, Multi-Object Manipulation, Stacking

I. INTRODUCTION

The growing field of Embodied AI is focused on creating autonomous systems that can physically interact with and modify their environments to achieve goals. A crucial aspect of this interaction is the ability to rearrange objects, a task identified as a canonical challenge for embodied agents [1]. This capability is fundamental to a wide range of applications, from industrial automation, such as sorting and packing on a production line [2], to domestic services like tidying a room [3]. The comprehensive nature of rearrangement, which unifies perception, planning, and manipulation, makes it a robust benchmark for progress in autonomous robotics.

The goal of rearrangement planning is to find a sequence of actions to move a set of objects from an initial arrangement to a target one [2]. This process requires a robotic system to first perceive the environment to establish the initial and target configurations. Subsequently, the planner must address the core challenge of objects obstructing each other’s target locations. It computes a sequence of pick-and-place actions, often using temporary buffer positions, to resolve these conflicts and

Human and Robot Interaction Laboratory, School of Electrical and Computer Engineering, University of Tehran, Tehran, Iran (e-mail: arman.barghi@ut.ac.ir, hosseini.hamed@ut.ac.ir, seraj.ghasemi@ut.ac.ir, m.t.masouleh@ut.ac.ir, akalhor@ut.ac.ir).

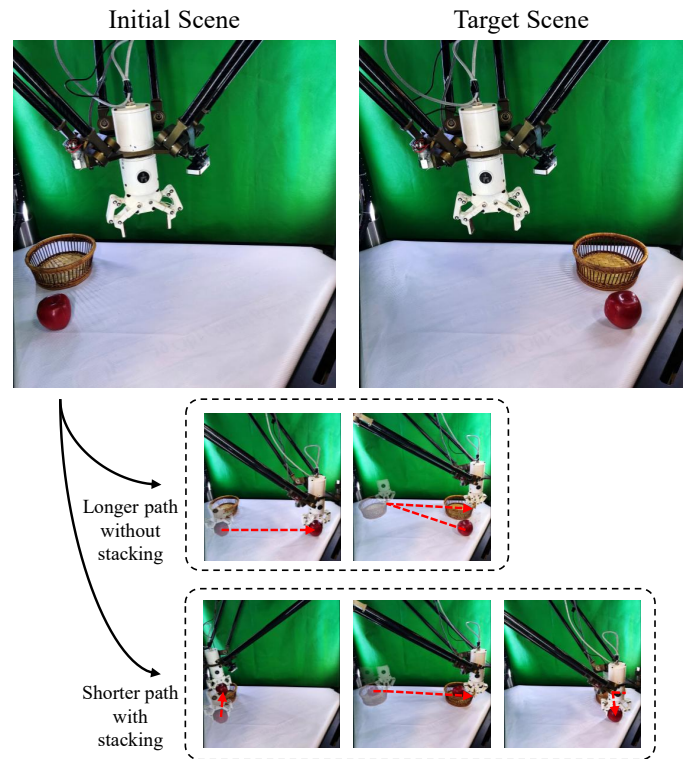


Fig. 1: A comparison of two rearrangement plans. The plan on the bottom uses dynamic stacking to minimize travel distance, resulting in a lower overall travel cost despite requiring a greater number of actions. The plan on the top, which does not use stacking, has a higher travel cost.

ensure that each object can be moved to its destination without collision. Once a complete plan is generated, it is passed to the robot for execution. The overall framework, from visual input to robot action, is illustrated in Fig. 2.

A key formulation of this challenge is the Tabletop Object Rearrangement with Overhand Grasps (TORO) problem, which seeks a plan that minimizes cost, primarily by reducing the number of pick-and-place actions [4]. The problem is fundamentally NP-hard, with its complexity stemming from object dependencies that arise when objects obstruct each other’s goal positions [4]. Resolving these conflicts requires using “buffers”—temporary locations for objects that are in the way. While finding a feasible plan is difficult, optimizing for cost-efficiency is even harder, as the selection of buffer locations directly impacts the total manipulator travel distance [5], [6]. Traditional approaches often struggle in

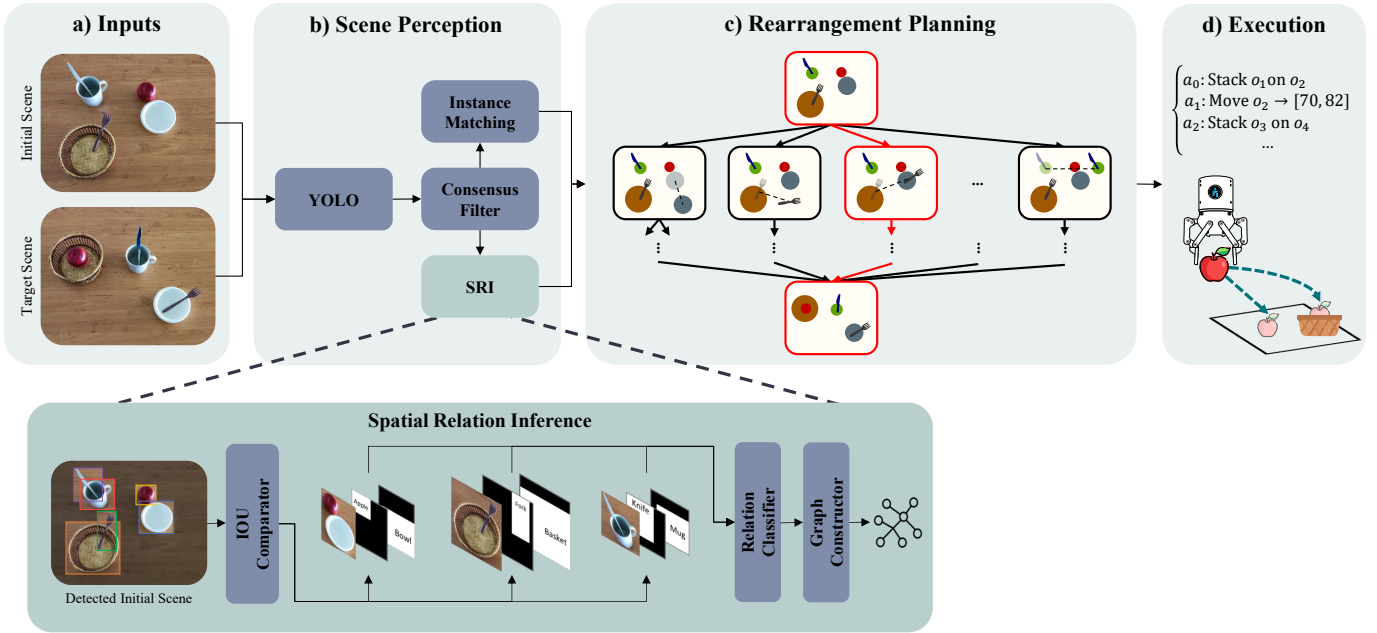


Fig. 2: Overall framework of the proposed robotic rearrangement system, illustrating the multi-stage pipeline from initial and target scene perception to rearrangement planning and execution.

high-density scenarios where limited buffer space is available, leading to limitations in both feasibility and plan quality.

In high-density scenarios, stacking objects can create valuable buffer space. Prior works have used this in several ways: as a tactical tool to free up a path in retrieval tasks [7], as a core strategy for buffering during rearrangement [8], or even as part of an optimal, long-term shelf layout [9]. However, a key limitation unites these approaches: the stacks are treated as static. Once an object is placed on top of another, the base object is locked in place.

This static approach is inefficient and unlike how humans approach complex organization. Humans often create temporary groups of items—like stacking bowls—and then transport the entire group in a single action, a highly efficient form of multi-object manipulation. Inspired by this, this paper introduces the Dynamic Buffer, a novel planning primitive that enables this strategy for robots. The core idea is to deliberately form stacks and relocate them by moving the base object. This transforms a series of single-object actions into a single, efficient multi-object move, significantly reducing manipulator travel distance. To the authors’ knowledge, this is the first work to treat stacks not merely as static buffers, but as dynamic, transportable units to improve cost-efficiency in a long-horizon rearrangement plan.

The principal contributions of this paper are twofold:

- Introduction of the *Dynamic Buffer*, a novel planning primitive that enables temporary stacks to be treated as movable units, thereby transforming stacking from a static buffering tool into a dynamic, transportable concept that improves cost-efficiency in rearrangement planning.
- Design and validation of an integrated rearrangement system that incorporates perception, object correspondence, and stacking-relationship detection to generate and

execute plans that effectively exploit the Dynamic Buffer primitive.

The remainder of this paper is structured as follows. Section II provides a comprehensive overview of related work in robotic object perception, rearrangement planning, and multi-object manipulation, followed by Section III, which explains the problem statement. Section IV details the proposed methodology, including the scene perception, search algorithm, expansion strategy, and plan refinement. Experimental validation and a thorough analysis of results are presented in Section V, followed by concluding remarks and future directions in Section VI.

II. RELATED WORKS

This section provides a comprehensive overview of existing research relevant to robotic object rearrangement planning. It begins by examining the foundational aspects of scene perception, followed by a detailed review of various rearrangement planning approaches, and concludes with a discussion on strategies for multi-object manipulation.

A. Scene Perception

A fundamental challenge in rearrangement planning is perceiving the environment to define the goal and represent the scene. The goal itself can be specified in various ways. It can be an explicit set of final object poses [5], [6], [8], an implicit objective function to optimize—such as a “tidiness score”—rather than a fixed final state [12], or a natural language command [13]. In some cases, a goal is not provided at all and must be generated from commonsense rules [14]. To reason about the scene, planners often use graph-based representations to capture object relationships. These can be

Table I: Comparison of robotic object rearrangement planning methods, highlighting buffering strategies, object-as-buffer usage (SS: Static Stacking, DS: Dynamic Stacking), placement decision logic, optimization objectives, and manipulator applicability.

| Paper | Buffering Method | Unoccupied Object Goal Strategy | Occupied Object Goal Strategy | Optimization Objective | Mobile Manip. |
|--------------------|---|---------------------------------|-------------------------------|----------------------------------|---------------|
| TORO [4] (2018) | External | Direct to Goal | To External Buffer | Cost-Eff. (Manip. Travel) | × |
| MCTS [2] (2020) | Internal (Unoccupied Space) | Direct to Goal | Move Obstructing Obj. | Feasibility | × |
| TRLB [5] (2022) | Internal (Unoccupied Space) | Direct to Goal | To Lazy Buffer | Cost-Eff. (Num. of Actions) | × |
| HetGNN [10] (2023) | Internal (Unoccupied Space) | Policy-Learned | Policy-Learned Action | Cost-Eff. (Action Type) | × |
| PMMR [11] (2024) | Internal (Unoccupied Space) | Prioritized Direct to Goal | To Sampled Buffer | Cost-Eff. (Obj. Travel) | × |
| ORLA* [8] (2024) | Internal (Unoccupied Space + SS) | Direct to Goal | To Lazy Buffer | Cost-Eff. (Manip. Travel) | ✓ |
| STRAP [6] (2025) | Internal (Unoccupied Space) | Direct to Goal | To Sampled Buffer | Cost-Eff. (Manip. Travel) | ✓ |
| This Work | Internal (Unoccupied Space + DS) | Prioritized Stacking | To Sampled Buffer | Cost-Eff. (Manip. Travel) | ✓ |

hierarchical, combining low-level geometric data with high-level symbolic relations like On(Can, Shelf) [15]; heterogeneous, using different node and edge types to capture rich semantics [10]; or structured to encode the task directly, where each node represents a corresponded start-goal object pair [16].

When the goal is provided as raw visual data, such as an image [2], [11], it introduces the critical subproblem of object matching. The robot must determine the correspondence between objects in the initial and target scenes. While many methods assume this correspondence is known, more realistic approaches must solve it as part of their process. To do so, works such as [10], [16], [17] integrate correspondence estimation directly into their perception pipeline.

B. Rearrangement Planning

Rearrangement planning is a core subfield of Task and Motion Planning (TAMP) that integrates task sequencing with motion generation [18]. Tasks are either retrieval-based, focused on accessing a single object [19], [20], or goal-oriented, where all objects have a target configuration. While goal-oriented problems span diverse domains like room-scale rearrangement [1], [21], [22] and confined spaces [23], this work focuses on tabletop manipulation, a challenge defined by dense clutter and high object dependency [2]. To provide a structured overview, Table I compares recent methods across the key aspects discussed below. To resolve object dependencies, planners use different buffering strategies. External buffers use a dedicated off-table area, with goals like minimizing total moves [4] or the number of running buffers [24]. More challenging are internal buffers, which use free on-table space but risk creating new blockages [5]. More recently, stacking has been used as a buffer, where objects themselves serve as temporary spots in dense scenes [8].

Planning approaches for rearrangement can be distinguished by their objective. Some methods focus primarily on finding a feasible solution without an explicit cost function. These include learning-based approaches that determine if a plan is achievable [16] and planners that use Monte Carlo Tree Search (MCTS) to find a valid sequence of actions [2]. In contrast, cost-efficient approaches aim to generate high-quality plans by optimizing a specific metric. However, the notion of "high-quality" differs across works. Some planners seek to minimize the number of object moves, either by reducing the problem

to finding a minimum Feedback Vertex Set (FVS) [4] or through specialized search [5]. Other works define cost based on action types (e.g., pushing is cheaper than picking) [10] or the total distance traveled by the objects themselves [11]. A more practical objective is minimizing the robot's total travel distance, as it strongly correlates with time and energy. Heuristic search algorithms like A^* are commonly used to find efficient solutions for this metric [6], [8].

A planner's placement strategy is key for efficiency. If a target is occupied, planners might move the blocking object [2], relocate the current object to a buffer [4], [6], or assign a buffer lazily [5], [8]. If the target is unoccupied, the default is to move directly to it. However, to find better long-term plans, some methods still evaluate other options [11]. This work introduces a novel strategy: prioritizing stacking even when the goal is free to enable more efficient multi-object moves later on, as illustrated in Fig. 1.

To scale rearrangement, research has moved beyond single stationary arms. One approach uses multi-arm systems to improve coordination and throughput [25]. However, for large tabletops where a single stationary arm cannot reach the entire workspace, the primary solution is a mobile manipulator [6], [8]. The main challenge then becomes the integrated planning of the mobile base and arm, where minimizing base travel distance is the key optimization objective.

C. Multi-Object Manipulation

The choice of manipulation primitive is critical for rearrangement. Actions are typically prehensile (grasping), non-prehensile (e.g., pushing), or hybrid. While non-prehensile actions can sort objects [26], they often lack the precision needed for cluttered scenes, where the high accuracy of prehensile grasping is essential [5], [8]. Hybrid methods combine these approaches, for instance by using suction to assist with pushing objects that are difficult to lift [11]. While these primitives are fundamental, scaling up efficiency requires moving beyond a one-object-at-a-time paradigm.

To overcome the inefficiency of single-object actions, research in multi-object manipulation shows a clear evolution toward more intelligent planning. The initial approach focused on the physics of the grasp itself, planning how to best pick up several objects that were already adjacent [27]. A subsequent step handled cases where objects were not yet grouped. In

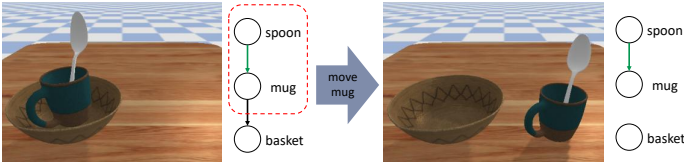


Fig. 3: The Dynamic Buffer concept in action: when a base object (mug) is moved, the stacked object (spoon) moves along with it, maintaining their relative stacking relationship, as also shown in the accompanying relational graphs.

what is called the “Busboy Problem,” the robot first performs setup actions—like stacking one item into another (“stack-grasp”)—to arrange objects into a compact, graspable configuration before lifting them as a single unit [28]. Building on this, the most recent approach adds a layer of semantic understanding, enabling a robot to first perceive existing stable stacks in the environment and then intelligently decide if it’s more efficient to move an entire stack at once rather than its individual items [29].

While these foundational works treat stacking as a tactic for aggregation or removal, recent methods have also used it for buffering in dense scenes [8]. However, these approaches typically treat stacks as **static**, preventing the base object from being moved. This work addresses this limitation by introducing the *Dynamic Buffer*, a new primitive where temporary stacks are actively created and taken apart within the workspace to strategically free up space. This fundamental shift allows for more flexible and cost-efficient planning. To demonstrate its effectiveness, this concept is integrated into the state-of-the-art, A^* -based STRAP planner [6] and a foundational MCTS-based planner focused on feasibility [2]. The approach is evaluated with both stationary and mobile manipulators and is benchmarked against the static stacking concept from ORLA* [8].

III. PROBLEM STATEMENT

The robotic object rearrangement problem involves transforming an initial configuration into a desired target configuration. This task begins with visual observations of both the initial and target scene images, denoted as I_{init} and I_{target} . A perception module processes these images to extract structured representations that describe the objects, their positions, and their pairwise relations. After establishing consistent correspondences between the objects in the two scenes, a unified set of object identifiers $\mathcal{V} = \{o_1, \dots, o_n\}$ is obtained, which serves as the basis for the state representation.

A state is defined as a valid and collision-free configuration of the environment, determined by the arrangement of objects together with the manipulator position. Formally, each state is represented as $s = (\mathcal{G}, p_m)$, where $\mathcal{G} = (\mathcal{V}, \mathcal{E})$ is a relational graph encoding the object arrangement and p_m denotes the manipulator’s position. The edges \mathcal{E} specify stacking relationships, with an edge e_{ij} indicating that object o_i is stacked on object o_j . The manipulator starts at a predefined home position $p_m^{(0)}$ and is assumed to return to this position $p_m^{(T)} = p_m^{(0)}$ upon task completion.

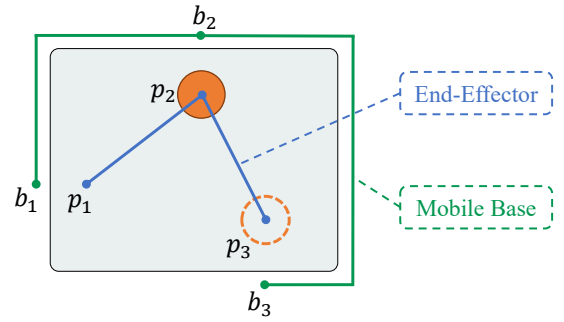


Fig. 4: Visual representation of travel cost of manipulation the orange object. The blue path indicates the EE travel, and the green path indicates the MB travel.

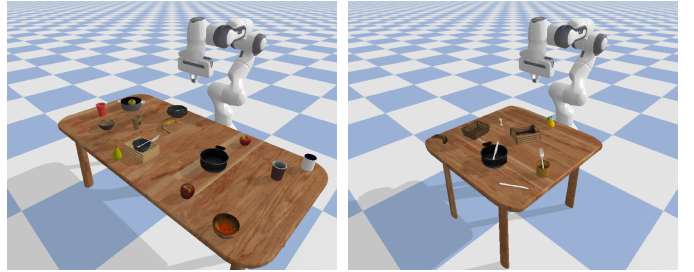


Fig. 5: The two manipulator configurations used in the simulation. (Left) A mobile manipulator is used for larger tables that require the robot’s base to move to reach all objects. (Right) A stationary manipulator is used for smaller tables where the base can remain fixed.

The goal state $s^{(T)}$ specifies the desired configuration of the objects. For each object, this goal can be defined either by an absolute target position or by a relative stacking relation with another object. The robotic rearrangement problem is therefore to compute a collision-free and cost-efficient plan that transforms the environment from the initial state $s^{(0)}$ to the target state $s^{(T)}$.

An action $a \in \mathcal{A}$, where \mathcal{A} is the set of all valid actions, results in the system transitioning to a new state $s' = \mathcal{T}(s, a)$ and incurring a cost $c(a)$, while the manipulator’s position p_m is updated with each action. In this framework, two action primitives can be performed on an object o_i :

- **Move:** Relocate o_i from its current position p_i to an unoccupied position p'_i .
- **Stack:** Place o_i from its current position p_i onto a stackable object o_j at position p_j whose top is clear, establishing a stacking relationship (represented by updating the edge $e_{ij} = 1$).

A core feature of this approach is the concept of a “Dynamic Buffer”: when an object o_i is moved to a new position, all objects stacked upon it (i.e., with an edge $e_{ji} = 1$, and their transitive dependents) move accordingly, maintaining their relative stacking relationships. This dynamic movement of stacked objects, exemplified by moving a cup containing a spoon (as depicted in Fig. 3), is utilized to achieve efficient rearrangement planning.

The objective is to minimize the cumulative travel cost

incurred by the manipulator throughout the action sequence required to reach the target state. While the total number of discrete actions can serve as a proxy, the manipulator’s total traveled distance (or travel cost) more accurately reflects real-world operational cost. This cost is measured in the XY plane, and its calculation depends on the robot’s configuration. For a stationary robot, the cost is based on End-Effector (EE) travel (blue path in Fig. 4). For a mobile robot, necessary for larger tables beyond a stationary arm’s reach, the cost is based on Mobile Base (MB) travel (green path in Fig. 4). These different manipulator configurations are further exemplified in Fig. 5. This comprehensive travel cost is a crucial metric. For example, a strategy like using a ‘Dynamic Buffer’ might involve more individual actions but can significantly lower the overall travel cost by moving grouped objects as a single unit, unlike rearranging them independently (Fig. 1).

The cost $c(a^{(t)})$ associated with the t -th action, which moves object o_i from $p_i^{(t)}$ to $p_i^{(t+1)}$, is calculated as follows:

$$c(a^{(t)}) = d(p_m^{(t)}, p_i^{(t)}) + d(p_i^{(t)}, p_i^{(t+1)}) + c_{pp} \quad (1)$$

The overall objective function to minimize the total cumulative cost $\mathcal{J}(\mathcal{P})$ for a action sequence \mathcal{P} from initial state $s^{(0)}$ to final state $s^{(T)}$ is:

$$\min_{\mathcal{P}} \mathcal{J}(\mathcal{P}) = \sum_{t=0}^{T-1} c(a^{(t)}) + d(p_m^{(T-1)}, p_m^{(0)}) \quad (2)$$

$$\text{s.t. } s^{(t+1)} = \mathcal{T}(s^{(t)}, a^{(t)}), \quad \forall t = 0, \dots, T-1 \quad (3)$$

where:

- $a^{(t)}$: Action applied at time t ;
- $d(x, y)$: Manipulator travel distance between position x and position y ;
- $p_m^{(t)}$: Manipulator’s position at time t ;
- $p_i^{(t)}$: Object o_i ’s position at time t ;
- $p_i^{(t+1)}$: Object o_i ’s next position after $a^{(t)}$;
- c_{pp} : Constant pick-and-place cost.

IV. SCENE REARRANGEMENT

This research develops an efficient sequence planning framework for robotic scene rearrangement tasks. Given initial and final scene configurations, the system autonomously determines a high-quality sequence of actions to transition between them. This is achieved through a multi-stage pipeline, detailed in the following subsections: scene perception for state representation, a search-based planner employing a novel heuristic and expansion strategy, and a final plan refinement stage to optimize the resulting action sequence.

A. Scene Perception

Accurate scene perception is fundamental for robotic manipulation, enabling robots to interpret their environment and the objects within it. The overall framework, from visual input to robot action, is illustrated in Fig. 2. Objects are assumed to belong to four functional groups defined by stacking properties:

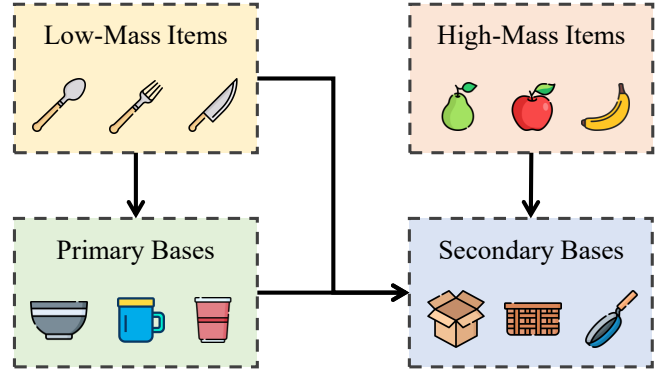


Fig. 6: Predefined object categories and their assumed stable stacking relationships. Arrows indicate that the object at the tail can be stably stacked on the object at the head.

- **Primary Bases:** containers such as boxes, pots, and baskets that can serve as a base for any other object group;
- **Secondary Bases:** containers such as bowls, mugs, and paper cups that can only support Low-Mass Items;
- **Low-Mass Items:** objects such as spoons, forks, and knives;
- **High-Mass Items:** objects such as apples, pears, and bananas that cannot be stacked on Secondary Bases due to instability.

Stacking stability is determined by a predefined lookup table, and each base is assumed to support only one item. While this restricts expressiveness, it ensures predictable, collision-free stacking. The four functional object groups and their assumed stable stacking relationships are illustrated in Fig. 6. Future work could instead learn or dynamically infer stacking feasibility.

For object detection, YOLOv5 [30] is employed to detect the 12 object classes corresponding to the functional groups introduced above. To refine the raw detections from the initial and target scenes, a **Consensus Filter** is applied. This filter’s purpose is to reconcile the two sets of detections by enforcing consistency between the views. It works by cleaning up duplicates and matching corresponding objects to generate a single, synchronized set of objects reliably found in both scenes. The **Instance Matching** module then establishes the final one-to-one correspondence required for planning, which is particularly important for classes with multiple instances. The cost for matching an object from the initial scene with one from the target scene is based on the Euclidean distance between the centers of their bounding boxes, b_i and b_j respectively:

$$C_{ij}^{\text{dist}} = \|\text{center}(b_i) - \text{center}(b_j)\|_2.$$

The Hungarian algorithm uses this cost to assign the most spatially coherent matches, resulting in two aligned and ordered object lists for the planner.

For spatial reasoning, the **Spatial Relation Inference (SRI)** module builds on the CNN-based architecture of [31]. A dataset of 604 real tabletop images containing kitchen objects

was collected, complemented by 2500 simulated scene pairs generated in PyBullet [32]. In the simulation, 12 object classes corresponding to the functional groups introduced above were defined, and stacking relations were randomly sampled under the same category-based rules. Both real and simulated datasets were used to train the relation detection module, while the simulated pairs were additionally employed in the rearrangement experiments. The CNN processes cropped regions of overlapping object pairs and predicts whether one object is stacked on another or whether no relation exists. These relations are then assembled into a scene graph representing the stacking structure, which is subsequently provided to the rearrangement planner.

B. Search Algorithm

As exhaustive methods are too time consuming, heuristic methods are feasible and useful to plan. The A^* algorithm, thus, is employed to find high-quality plans for the rearrangement task. This algorithm, building upon its application in [6], extends its core functionality with action primitives (move and stack) defined in the problem formulation. Within the A^* search, each state s is represented as a node, and valid actions a are directed edges transitioning between states. The algorithm explores states by prioritizing those with the lowest estimated total cost $f(s) = g(s) + h(s)$, where $g(s)$ is cost-to-come which is the cumulative cost from the initial state and $h(s)$ is the estimated cost-to-go which is cumulative cost from the current state reaching to the target state. This process continues until the target state $s^{(T)}$ is reached, ensuring a high-quality sequence of actions that minimizes the overall cost given an admissible heuristic. The search for the optimal path is further accelerated by use of a heuristic function. The A^* algorithm, using a priority heap, explores the search space by expanding the most promising nodes first.

Heuristic Function with Stacking Awareness: Defining a proper heuristic function $h(s)$ is critical for ensuring the efficiency and optimality guarantees of A^* . The baseline heuristic from [6] considers the distance of objects in current state to their goal positions and associated pick-and-place costs. However, directly applying this heuristic is insufficient when incorporating stacking primitives, as stacking can lead to a lower true cost than a direct move (see Fig. 1). This could make the heuristic non-admissible, meaning it might overestimate the true cost to the goal. In order to guarantee that A^* finds an optimal solution, the heuristic must be admissible [33]. Therefore, a novel heuristic is introduced that accounts for stacking capabilities. For each object o_i , its estimated cost-to-go $h_i(s^{(t)})$ is the minimum of its distance to its target position and the distances to all candidate base objects it could stack upon. This ensures the heuristic remains an underestimate of the true optimal cost, thereby preserving A^* 's admissibility. The full heuristic is defined mathematically

as:

$$h(s^{(t)}) = \sum_{i=1}^n h_i(s^{(t)}) + n \cdot c_{pp}, \quad (4)$$

$$h_i(s^{(t)}) = \min \left(d(p_i^{(t)}, p_i^{(T)}), \{d(p_i^{(t)}, p_j^{(t)}) + c_{pp}\}_{o_j \in \mathcal{C}_i} \right), \quad (5)$$

where n is the number of remaining objects that are not at their goal. The set of candidate bases, \mathcal{C}_i , includes all objects that are stable for o_i to be stacked on, whose tops are clear. The distance function, $d(x, y)$, represents the manipulator's travel cost as defined in Section III, using either the EE or MB travel distance depending on the robot configuration.

To enhance the overall planning efficiency and handle long-horizon problems, ensuring a feasible plan is available at each step, the "Goal Attempting" strategy introduced by STRAP [6] is adopted as a high-speed feasible planner, capable of generating a quick plan from the current state to the goal within a given time budget. In this paper, Goal Attempting functionality is powered by an algorithm based on the MCTS planner [2], into which the dynamic stacking primitives are integrated. This MCTS component is designed to find a fast feasible plan, and for this purpose, it allows manipulating a similar object consecutively. This can lead to plans of lower quality; however, these immediate redundancies are efficiently addressed by the first stage of the refinement process (Section IV-D).

C. Expanding Strategy

In the A^* search, the method for generating successor states and deciding an object's next placement is crucial. For each object, its goal is defined either by a target position or by a stacking relationship with another object in the target scene. The expansion strategy, detailed in Algorithm 1, manages the search's branching factor by limiting successor states for each object to a predefined buffer count N_{buf} . This budget is then partitioned such that a majority (e.g., 60%) is allocated to potential `stack` actions, while the remainder is dedicated to `move` actions.

The action generation process for an object o_k begins with exploring stacking opportunities by creating `stack` actions from a random sample of its valid base objects, O_k (Lines 5–7). The generation of complementary `move` actions is guided by the goal's availability, a process that starts by identifying the set of all valid collision-free placements, P_k (Line 9). If the goal position is occupied (i.e., $p_k^{(T)} \notin P_k$), alternative placements are sampled from P_k (Line 10–11). If the goal is available, however, a strong goal-oriented bias is applied, and the sole `move` action generated is the one that places the object directly at its target (Line 14). This dual approach allows the A^* search to evaluate the cost-effectiveness of both direct-to-goal actions and intermediate stacking maneuvers that may be more efficient in the long run.

Action Generation and Validation: The validity of actions is ensured through a two-step process. For a `move` action, the set of all collision-free locations is identified using a Summed-Area Table (SAT), also known as an integral image [34]. This technique is applied to the multi-label occupancy map

Algorithm 1: The Proposed Expansion Strategy for Generating Successor Actions.

Input: $S = (s^{(t)}, s^{(T)})$: The current and target arrangements.

Input: N_{buf} : The number of buffer slots per object.

Result: A_{valid} : A set of valid actions.

```

1  $O_{\text{rem}} \leftarrow \{o_i \text{ not in its goal}\}$ 
2  $A_{\text{valid}} \leftarrow \emptyset$ 
3  $N_{\text{stack}} \leftarrow \max(\lfloor 0.6 \cdot N_{\text{buf}} \rfloor, 1)$ 
4 for each  $o_k$  in  $O_{\text{rem}}$  do
5    $O_k \leftarrow \text{getValidStackTargets}(o_k)$ 
6    $O'_k \leftarrow \text{Sample}(O_k, N_{\text{stack}})$ 
7    $A_{k,\text{stack}} \leftarrow \{\text{stack}(o_k, o_j) \mid o_j \in O'_k\}$ 
8    $N_{\text{move}} \leftarrow N_{\text{buf}} - |A_{k,\text{stack}}|$ 
9    $P_k \leftarrow \text{getValidPositions}(o_k)$ 
10  if  $p_k^{(T)} \notin P_k$  then
11     $P'_k \leftarrow \text{Sample}(P_k, N_{\text{move}})$ 
12  end
13  else
14     $P'_k \leftarrow \{p_k^{(T)}\}$ 
15  end
16   $A_{k,\text{move}} \leftarrow \{\text{move}(o_k, p) \mid p \in P'_k\}$ 
17   $A_{\text{valid}} \leftarrow A_{\text{valid}} \cup A_{k,\text{stack}} \cup A_{k,\text{move}}$ 
18 end
19 return  $A_{\text{valid}}$ 

```

to allow for the rapid validation of all possible placements for a given object's footprint in a single, efficient pass. For a `stack` action, the set of feasible base objects is determined by looping through all objects in the environment. The stability of a stacking configuration is determined by a predefined lookup table.

D. Plan Refinement

To enhance the quality of generated plans, a two-stage refinement process is applied, aiming to eliminate redundant actions, ensure action sequence coherence, and optimize buffer locations. The two stages are as follows:

Redundancy Pruning: This first stage rigorously eliminates redundant actions from the planner's output while preserving plan feasibility. This is achieved by removing consecutive operations that manipulate the same object, keeping only the final relevant action. Additionally, non-consecutive redundancies are identified and skipped by checking if an action produces any tangible change to an object's intended state. This comprehensive pruning results in a more concise, efficient, and feasible plan.

Buffer Optimality: The second stage focuses on optimizing the locations of temporary buffers within a refined action sequence. This is particularly crucial for objects manipulated multiple times, where an initial placement into a temporary location is followed by a subsequent transfer to its final goal or another buffer. The objective is to identify the most cost-efficient location for such buffered objects throughout their

trajectory. Unlike prior work that primarily considers basic movements for static buffer optimization [6], this stage explicitly incorporates stacking primitives. As previously discussed, stacking an object can create a dynamic buffer, or unoccupied locations can act as static buffers. This allows the refinement process to leverage the advantages of both approaches. Both static and dynamic buffers are illustrated in Fig. 7.

As depicted in Fig. 7a, for each object o_k that is temporarily buffered (first manipulated at index b to a buffer, and then again at index i), the optimal buffer position is re-evaluated. This involves minimizing the cumulative manipulator travel cost associated with both manipulations of o_k . This cost incorporates four key distances:

- 1) Manipulator travel to place o_k from its pick position to the buffer position p at index b ;
- 2) Manipulator travel from p to the pick position of the next object in the sequence at index $b + 1$;
- 3) Manipulator travel to pick o_k from its buffer location at index i ;
- 4) Manipulator travel to place o_k at its target position or another buffer at index i .

Given an action sequence \mathcal{P} , the optimization objective to find the best static buffer p^* is:

$$\min_{p \in P_k} \left(|\mathcal{P}_{\text{pick}}^{(b)} - p| + |p - \mathcal{P}_{\text{pick}}^{(b+1)}| + |\mathcal{P}_{\text{place}}^{(i-1)} - p| + |p - \mathcal{P}_{\text{place}}^{(i)}| \right) \quad (6)$$

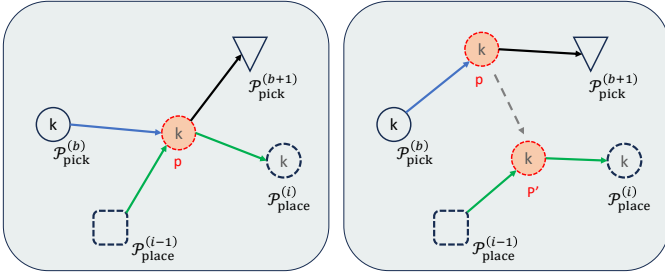
Here, P_k denotes the set of unoccupied collision-free locations for o_k . For dynamic buffers, which involve stacking object o_k onto a base object o_j , the cost calculation must account for the dynamic nature of the buffer. Since the position of the base object o_j can change between the manipulations of o_k at indices b and i , the cost function considers not only the original buffer location $p_j^{(b)}$ but also its potentially different subsequent location $p_j^{(i)}$, as depicted in Fig. 7b. This is in contrast to static buffers, whose positions remain fixed. The optimization objective to find the best dynamic buffer o_j^* is:

$$\min_{o_j \in C_k} \left(|\mathcal{P}_{\text{pick}}^{(b)} - p_j^{(b)}| + |p_j^{(b)} - \mathcal{P}_{\text{pick}}^{(b+1)}| + |\mathcal{P}_{\text{place}}^{(i-1)} - p_j^{(i)}| + |p_j^{(i)} - \mathcal{P}_{\text{place}}^{(i)}| \right) \quad (7)$$

Here, C_k is the set of valid base objects for o_k whose tops remain clear from index b to i . This dynamic buffer cost is then compared against the cost of using an optimal static buffer location. Based on whichever option yields the minimal cost, action b is updated to either move the object to the best location p^* or to stack it on the chosen object o_j^* . This comprehensive refinement leverages stacking for improved plan quality.

V. RESULTS

This section presents the experimental validation and analysis of the proposed stacking approach for object rearrangement planning. The performance of the integrated system is evaluated in three distinct parts: a comprehensive algorithm



(a) Refinement proposed in [6] (b) The proposed refinement which finds the best static buffer. which takes into consideration dynamic buffers as well as static buffers.

Fig. 7: Blue is the path traveled by manipulator in the action index b for moving object k to a buffer p ; Green is the path traveled by manipulator in the action index i for moving object k from buffer p to another location; Red shows the buffer candidates.

comparison against several baselines, an analysis of key components and parameters within the framework, and a final full pipeline experiment conducted in both simulation and the real world.

A. Algorithm Comparison

To validate the effectiveness of the Dynamic-Stacking (DS) approach, its performance is compared against several baseline methods, representing both traditional Non-Stacking (NS) and Static-Stacking (SS) strategies. The following algorithms are evaluated:

MCTS: The standard MCTS planner [2], used for finding feasible rearrangement plans.

MCTS+DS: The proposed DS approach integrated into the MCTS planner.

STRAP: The A^* planner from [6], used for planning high-quality rearrangement sequences. This planner employs a Goal-Attempting mechanism, for which an MCTS planner is utilized internally.

STRAP+SS: The SS approach, representing existing stacking methods (e.g., as conceptualized in ORLA* [8]), integrated into the STRAP planner.

STRAP+DS: The proposed DS approach integrated into the STRAP planner.

For a fair comparison with baselines, which do not support pre-existing stacking, initial and target arrangements are generated without stacking relations. In this context, stacking primitives are exclusively used for intermediate buffering during the planning process. For each number of objects n , 40 random scene pairs were generated, and one trial was executed per pair. Each trial is subject to a 6-minute time limit to find a cost-efficient solution. Regardless of the success rate, the reported performance metrics—average travel cost, average number of actions, and average manipulation time—are evaluated over successful trials to remain consistent with previous works [6]. Travel cost is considered the primary metric, as it comprehensively quantifies both manipulator travel distances and pick-and-place operations. To ensure a consistent experimental

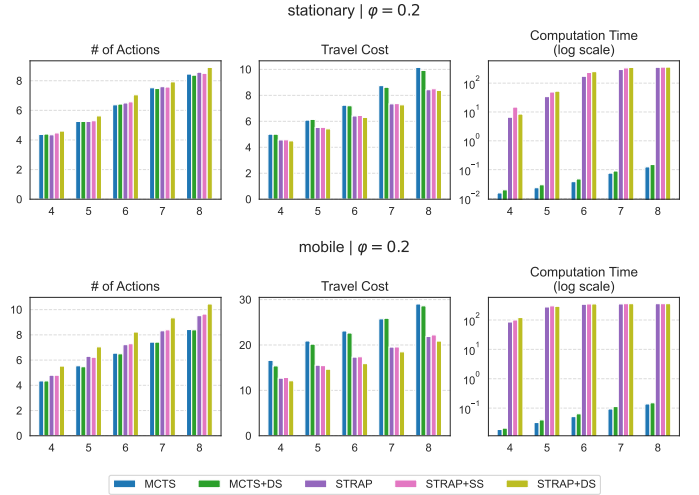


Fig. 8: Results for low-density scenes ($\varphi = 0.2$). The horizontal axis represents the number of objects in the scene. The top row illustrates performance for the stationary manipulator, while the bottom row presents the corresponding metrics for the mobile manipulator.

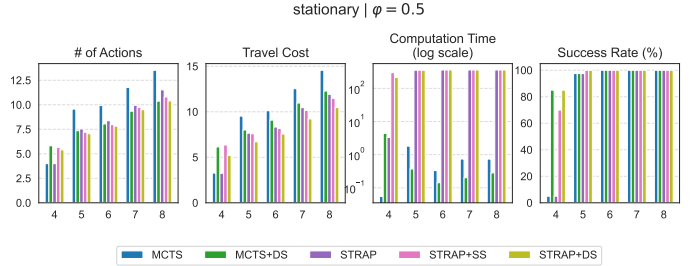


Fig. 9: Results for high-density scenes ($\varphi = 0.5$). The horizontal axis represents the number of objects in the scene. The plots display algorithm performance for the stationary manipulator in these challenging environments.

setup, uniformly sized objects are used. The scene density φ is then defined as the ratio of the total object footprint area $\sum_{o \in \mathcal{O}} S(o)$ to the total table area S_T [8], where $S(o)$ is the footprint size of object o . The table dimensions are 1×1 meters for stationary mode and 1×2 meters for mobile mode, and manipulator movement costs are normalized by the width of the table. Furthermore, a pick-and-place cost c_{pp} of 0.2 (one fifth of traveling the table's width) is applied per action.

To provide a robust assessment of performance that accounts for varying success rates and to enable a direct comparison of algorithms across different numbers of objects, the Expected Succeeded Cost (ESC) is defined as the average cost of successful trials divided by the success rate:

$$\text{ESC}(n) = \frac{\text{Average Cost of Trials}(n)}{\text{Success Rate}(n)} \quad (8)$$

In scenarios with 100% success rate, ESC simplifies to the average cost of successful trials. For an aggregate measure across all evaluated object counts, the Overall Performance

Table II: Comparison of algorithm performance across different scenarios. OPS and PIR are presented for each algorithm, covering stationary (EE) and mobile (MB) manipulators in low ($\varphi = 0.2$) and high ($\varphi = 0.5$) density scenes.

| Manip. | φ | Metrics | MCTS | | STRAP | | |
|--------|-----------|---------|-------|--------|-------|--------|---------------|
| | | | NS | DS | NS | SS | DS |
| EE | 0.2 | OPS | 7.45 | 7.38 | 6.46 | 6.49 | 6.37 |
| | | PIR | - | 0.92% | - | -0.46% | 1.31% |
| MB | 0.2 | OPS | 23.08 | 22.55 | 17.40 | 17.5 | 16.41 |
| | | PIR | - | 2.30% | - | -0.61% | 5.69% |
| EE | 0.5 | OPS | 11.75 | 10.14 | 9.64 | 9.35 | 8.49 |
| | | PIR | - | 13.72% | - | 2.96% | 11.89% |

Score (OPS) of an algorithm is defined as the mean of its ESC values, given in Eq. (8), over all relevant n :

$$\text{OPS} = \frac{1}{|\mathcal{N}|} \sum_{n \in \mathcal{N}} \text{ESC}(n) \quad (9)$$

where \mathcal{N} is the set of evaluated object counts. To quantify performance improvements between algorithms, the Performance Improvement Rate (PIR) of algorithm B over algorithm A by the metric of OPS represented in Eq. (9) is calculated as:

$$\text{PIR}(B \text{ over } A) = \frac{\text{OPS}(A) - \text{OPS}(B)}{\text{OPS}(A)} \times 100\% \quad (10)$$

The performance comparison across all algorithms and scenarios is shown in a combination of figures and a table. The results in Fig. 8 and Fig. 9 illustrate the performance trends, while Table II provides a numerical summary of the OPS and PIR for each algorithm. Fig. 8 shows results for both stationary and mobile manipulators, while the computationally expensive nature of high-density problems limits the analysis in Fig. 9 to the stationary manipulator only. It should be noted that for low-density scenarios, a universal 100% success rate was achieved by all algorithms, largely owing to the "Goal Attempting" mechanism. Consequently, ESC for these scenarios simplifies to the average cost.

For low-density scenarios ($\varphi = 0.2$) in Fig. 8, stacking on MCTS (MCTS+DS) does not yield a significant improvement in performance compared to baseline MCTS, as MCTS primarily focuses on feasibility, and complex buffering is less critical in low-density settings. For the stationary manipulator (Fig. 8 top), STRAP+DS demonstrates a PIR of 1.31% in cost over baseline STRAP. This is reflected in the OPS values in Table II (6.46 for STRAP vs. 6.37 for STRAP+DS). In contrast, for the mobile manipulator (Fig. 8 bottom), the benefits of dynamic stacking are more pronounced. STRAP+DS achieves a PIR of 5.69% in cost over baseline STRAP, as seen in Table II (17.40 for STRAP vs. 16.41 for STRAP+DS). This improvement in cost for STRAP+DS in both stationary and mobile scenarios is accompanied by an increase in the average number of actions. This trend is expected, since in larger mobile workspaces, dynamic stacking allows grouped transfers that can reduce costs despite requiring more actions. In both stationary and

mobile scenarios, STRAP+SS shows no notable difference in performance compared to baseline STRAP.

High-density scenarios ($\varphi = 0.5$) pose significant challenges, particularly for algorithms lacking stacking capabilities, as free buffer space can become extremely scarce, rendering some problems infeasible. It should be noted that while the work of [6] did not evaluate performance in such high-density environments, this paper's algorithms are specifically tested under these conditions. In these challenging environments, the limited available space severely impacts success rates for non-stacking algorithms. For instance, the low average cost for STRAP at $n = 4$ is misleading, as it is derived from only 5% successful trials (2 out of 40 scenarios). Therefore, OPS is used for comparisons where relevant n values are from 5 to 8, and the 4-object scenario is excluded from this aggregate analysis due to its extremely low success rates for non-stacking methods, which can significantly skew comparative metrics and make the comparison unfair.

From Fig. 9, it can be inferred that stacking methods generally outperform non-stacking methods in high-density scenarios. This is supported by the data in Table II, which shows consistently lower OPS values for stacking methods. Here, STRAP+DS demonstrates significant advantages, achieving both lower travel cost and fewer actions. Furthermore, STRAP+SS provides a modest PIR of 2.96% over the STRAP baseline. Most notably, STRAP+DS achieves a PIR of 11.89% over the STRAP baseline in terms of cost, with its final OPS (8.49) being substantially lower than all other planners. This strongly indicates that Dynamic Stacking is vastly beneficial in high-density rearrangement tasks.

B. Component and Parameter Analysis

This section presents a detailed analysis of the planning framework's key components and parameters. The impact of the post-processing refinement stages is first studied, followed by an evaluation of the effect of the number of buffers used in the search algorithm. This analysis is crucial for understanding the contributions of each component to the overall performance and for justifying the parameter choices made in the main experiments.

1) *Refinement Study*: Table III illustrates the impact of the proposed plan refinement methods. For each entry, the OPS of the refined algorithm is presented in parentheses, followed by the PIR over its unrefined counterpart. In less challenging, low-density scenarios ($\varphi = 0.2$), dynamic refinement yields only marginal improvements over static refinement across all algorithms and manipulator types, indicating that initial plans are already quite efficient. The benefits of dynamic refinement are more pronounced in high-density scenarios ($\varphi = 0.5$), where it consistently provides a significantly higher PIR across all baselines. For example, applying dynamic refinement to MCTS results in a 12.06% improvement, substantially outperforming the 7.39% from static refinement.

It is notable that while the PIR values for STRAP+DS are lower compared to other variants, its final OPS remains superior. This demonstrates that the STRAP+DS planning algorithm's primary search already incorporates efficient stack-

Table III: Comparison in travel cost achieved by applying refinement methods. Values are presented as (OPS) and PIR% for each algorithm, where OPS is the overall performance score after refinement. "Static" rows show PIR from applying refinement with only static buffers (based on [6]); "Dynamic" rows show PIR from applying full refinement (incorporating dynamic buffers).

| Manip. | φ | Refine | MCTS | | STRAP | | |
|--------|-----------|---------|---------|---------|---------|---------|---------|
| | | | NS | DS | NS | SS | DS |
| EE | 0.2 | Static | (7.11) | (7.10) | (6.41) | (6.43) | (6.35) |
| | | | 4.52% | 3.84% | 0.74% | 0.84% | 0.43% |
| | | Dynamic | (7.10) | (7.09) | (6.41) | (6.43) | (6.35) |
| | | | 4.64% | 3.93% | 0.80% | 0.94% | 0.43% |
| MB | 0.2 | Static | (22.16) | (21.82) | (17.18) | (17.29) | (16.28) |
| | | | 4.00% | 3.22% | 1.21% | 1.18% | 0.74% |
| | | Dynamic | (22.11) | (21.81) | (17.16) | (17.21) | (16.28) |
| | | | 4.22% | 3.27% | 1.33% | 1.65% | 0.74% |
| EE | 0.5 | Static | (10.88) | (9.67) | (9.34) | (9.16) | (8.42) |
| | | | 7.39% | 4.61% | 3.01% | 2.08% | 0.88% |
| | | Dynamic | (10.33) | (9.37) | (9.14) | (8.96) | (8.40) |
| | | | 12.06% | 7.61% | 5.12% | 4.17% | 1.06% |

ing strategies, leading to high-quality initial plans that require less post-processing optimization. Therefore, even with a smaller PIR from refinement, STRAP+DS maintains its superior overall performance, leaving less room for further improvement.

2) *Parameter Study*: A study is conducted on the number of buffers utilized in the tree search, a key parameter for balancing exploration and efficiency. The impact of this parameter on performance is presented in Table IV, showing the PIR of STRAP+DS over STRAP. As defined in the methodology, a fixed ratio of dynamic to static buffers is maintained. The PIR peaks at 4 buffers (5.69%), which was consequently chosen as the default value for the main experiments. PIR is slightly reduced for 6 and 8 buffers, and significantly reduced for 10 buffers. This indicates that while increasing the number of buffers expands the search space, it does not necessarily lead to proportionally better plans, and can introduce inefficiencies due to the increased computational cost of exploring less optimal buffer choices. This highlights the importance of carefully selecting the number of buffers to balance search cost and plan quality.

C. Full Pipeline Experiment

The full pipeline, from visual input to robot execution, was evaluated in a more realistic setting than the algorithm comparisons. These experiments, which utilized general-shaped objects and included scenarios with pre-existing stacking relationships, serve to validate the robustness of the full system. The system's inputs were limited to two RGB images representing the initial and target scenes. The visual perception system achieved an accuracy of 92.42% on the real test set and 98.26% on the simulation test set, demonstrating strong

Table IV: Parameter study on the number of buffers. OPS and PIR for STRAP and STRAP+DS are presented as a function of the number of buffers. The results are for the mobile manipulator in low-density scenarios ($\varphi = 0.2$).

| Number of Buffers | OPS | | PIR |
|-------------------|-------|----------|-------|
| | STRAP | STRAP+DS | |
| 3 | 17.45 | 16.57 | 5.02% |
| 4 | 17.40 | 16.41 | 5.69% |
| 6 | 17.34 | 16.44 | 5.14% |
| 8 | 17.42 | 16.48 | 5.42% |
| 10 | 17.41 | 16.62 | 4.54% |

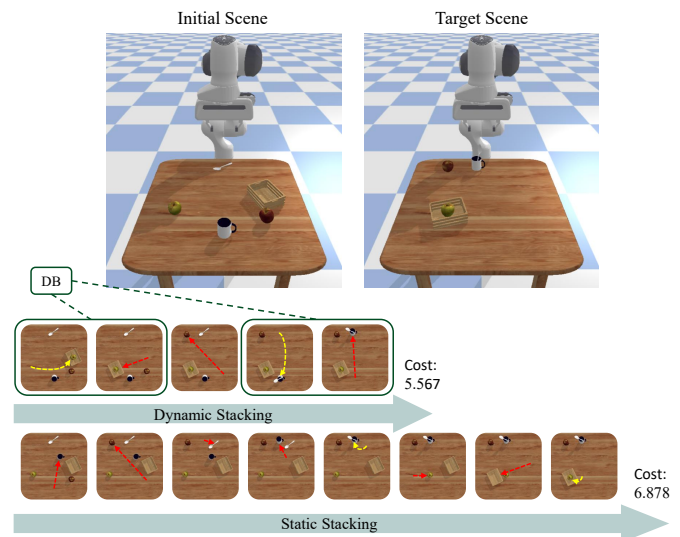


Fig. 10: A comparison of rearrangement plans using Static vs. Dynamic Stacking for a scene with pre-existing stacks. Dynamic Stacking allows objects like the box and mug to be used as movable 'dynamic buffers', resulting in a more efficient, lower-cost plan as shown.

performance across both domains and contributing to the system's robustness in real-world scenarios.

1) *Simulation Results*: The system was evaluated on 40 rearrangement tasks in a simulation environment, with each task composed of 10 random objects. These experiments were conducted using a Franka Emika Panda manipulator model [35] within the PyBullet physics engine [32]. The system successfully solved 39 out of 40 tasks, utilizing an average of 7.6 action steps for successful runs.

A specific simulation was examined to illustrate the fundamental difference between the dynamic and static stacking approaches, particularly in scenarios with pre-existing stacks. Static stacking primitives do not permit the relocation of an object that serves as a base for another, which constrains the available planning options. In contrast, the dynamic stacking approach allows an entire stack to be moved by manipulating its base object. This key capability is highlighted in Fig. 10. The figure demonstrates how leveraging an existing stack as

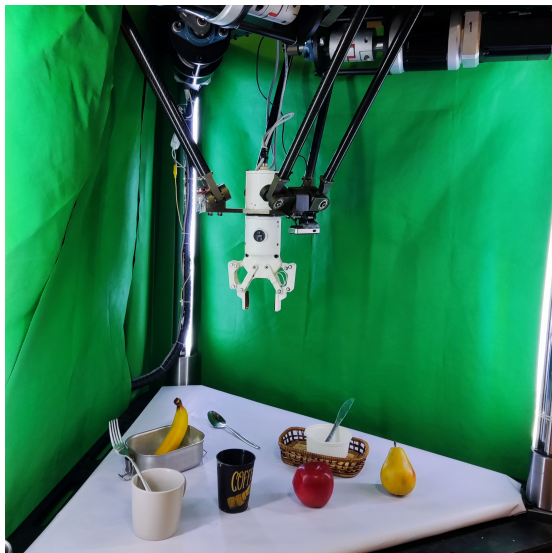


Fig. 11: The real-world experimental setup. The delta robot is shown preparing to perform a rearrangement task on the tabletop.

a single movable unit can lead to a more efficient plan with a significantly lower travel cost compared to the sequence of actions available to a static stacking approach.

2) *Real-World Results:* Real-robot experiments were performed using a custom-built delta robot described in [36]. An overview of the real-world setup is shown in Fig. 11. The system was evaluated on 20 rearrangement tasks, each composed of 5 objects. Of the 20 experiments, 18 were successful. For successful tasks, the system used an average of 5.1 action steps for execution. The few failures observed in both the simulation and real-world experiments stemmed from a common source, namely errors in the visual perception system. These issues typically involved incorrectly estimated object counts, mismatches between source and target objects, or the misclassification of stacking relations. The implementation code and supplementary experimental videos are available at the project repository.¹

VI. CONCLUSION

This paper introduced a novel approach to tabletop rearrangement planning by incorporating a Dynamic Buffer concept. This method, inspired by human strategies, enables multi-object manipulation by allowing temporary object stacks to be dynamically relocated, thus creating flexible, non-fixed buffer locations. This work demonstrates that integrating dynamic stacking into rearrangement planners yields significant benefits. The experimental results showed that this approach substantially enhances plan quality and efficiency. A cost reduction of 11.89% was achieved in challenging, high-density scenarios, while a 5.69% cost reduction was observed for large table mobile manipulation in low-density settings. These findings highlight that dynamic buffering is not only a crucial strategy for ensuring feasibility in environments with limited

buffer space but also a powerful technique for achieving cost-efficiency even when stacking is not strictly necessary. This research provides a solid foundation for advancing dynamic, multi-object manipulation in complex and constrained environments.

REFERENCES

- [1] D. Batra, A. X. Chang, S. Chernova, A. J. Davison, J. Deng, V. Koltun, S. Levine, J. Malik, I. Mordatch, R. Mottaghi, M. Savva, and H. Su, “Rearrangement: A challenge for embodied ai,” 2020.
- [2] Y. Labbe, S. Zagoruyko, I. Kalevtykh, I. Laptev, J. Carpentier, M. Aubry, and J. Sivic, “Monte-carlo tree search for efficient visually guided rearrangement planning,” *IEEE Robotics and Automation Letters*, 2020.
- [3] J. Wu, R. Antonova, A. Kan, M. Lepert, A. Zeng, S. Song, J. Bohg, S. Rusinkiewicz, and T. Funkhouser, “Tidybot: Personalized robot assistance with large language models,” *Autonomous Robots*, 2023.
- [4] S. D. Han, N. M. Stiffler, A. Krontiris, K. E. Bekris, and J. Yu, “Complexity results and fast methods for optimal tabletop rearrangement with overhand grasps,” *The International Journal of Robotics Research*, vol. 37, no. 13-14, pp. 1775–1795, dec 2018.
- [5] K. Gao, D. Lau, B. Huang, K. E. Bekris, and J. Yu, “Fast high-quality tabletop rearrangement in bounded workspace,” in *2022 International Conference on Robotics and Automation (ICRA)*, 2022, pp. 1961–1967.
- [6] J. Hu, J. Szczekulski, S. Peddabomma, and H. I. Christensen, “Planning for tabletop object rearrangement,” in *2025 IEEE International Conference on Robotics and Automation (ICRA)*, 2025, pp. 11 889–11 895.
- [7] J. Lee, U. Rakhman, C. Nam, S. Kang, J. Park, and C. Kim, “High dimensional object rearrangement for a robot manipulation in highly dense configurations,” *Intelligent Service Robotics*, vol. 15, no. 5, pp. 649–660, 2022.
- [8] K. Gao, Zhaxizhuoma, Y. Ding, S. Zhang, and J. Yu, “Orla*: Mobile manipulator-based object rearrangement with lazy a star,” 2024.
- [9] L. Y. Chen, H. Huang, and K. Goldberg, “Optimal arrangement and rearrangement of objects on shelves to minimize robot retrieval cost,” *IEEE Transactions on Automation Science and Engineering*, vol. 21, no. 3, pp. 2184–2198, 2024.
- [10] X. Lou, H. Yu, R. Worobel, Y. Yang, and C. Choi, “Adversarial object rearrangement in constrained environments with heterogeneous graph neural networks,” in *2023 IEEE/RSJ International Conference on Intelligent Robots and Systems (IROS)*, 2023, pp. 1008–1015.
- [11] B. Huang, X. Zhang, and J. Yu, “Toward optimal tabletop rearrangement with multiple manipulation primitives,” in *2024 IEEE International Conference on Robotics and Automation (ICRA)*, 2024, pp. 10 860–10 866.
- [12] H. Kee, W. Oh, M. Kang, H. Ahn, and S. Oh, “Tidiness score-guided monte carlo tree search for visual tabletop rearrangement,” *IEEE Robotics and Automation Letters*, vol. 10, no. 10, pp. 10 090–10 097, 2025.
- [13] H. Chang, K. Gao, K. Boyalakuntla, A. Lee, B. Huang, J. Yu, and A. Boularias, “Lgmcts: Language-guided monte-carlo tree search for executable semantic object rearrangement,” in *2024 IEEE/RSJ International Conference on Intelligent Robots and Systems (IROS)*, 2024, pp. 13 607–13 612.
- [14] G. Zhai, X. Cai, D. Huang, Y. Di, F. Manhardt, F. Tombari, N. Navab, and B. Busam, “Sg-bot: Object rearrangement via coarse-to-fine robotic imagination on scene graphs,” in *2024 IEEE International Conference on Robotics and Automation (ICRA)*. IEEE, 2024, pp. 4303–4310.
- [15] Y. Zhu, J. Tremblay, S. Birchfield, and Y. Zhu, “Hierarchical planning for long-horizon manipulation with geometric and symbolic scene graphs,” in *2021 IEEE International Conference on Robotics and Automation (ICRA)*. IEEE, 2021, pp. 6541–6548.
- [16] A. H. Qureshi, A. Mousavian, C. Paxton, M. Yip, and D. Fox, “Nerp: Neural rearrangement planning for unknown objects,” in *Proceedings of Robotics: Science and Systems*, Virtual, July 2021.
- [17] K. Xu, Z. Zhou, J. Wu, H. Lu, R. Xiong, and Y. Wang, “Grasp, see, and place: Efficient unknown object rearrangement with policy structure prior,” *IEEE Transactions on Robotics*, vol. 41, pp. 464–483, 2025.
- [18] C. R. Garrett, R. Chitnis, R. Holladay, B. Kim, T. Silver, L. P. Kaelbling, and T. Lozano-Pérez, “Integrated task and motion planning,” *Annual Review of Control, Robotics, and Autonomous Systems*, vol. 4, no. 1, pp. 265–293, may 2021.

¹<https://github.com/armanbarghi/DBRP-Code>

- [19] M. Kang, J. Kim, H. Kee, and S. Oh, "Object rearrangement planning for target retrieval in a confined space with lateral view," in *2023 IEEE/RSJ International Conference on Intelligent Robots and Systems (IROS)*, 2023, pp. 2004–2009.
- [20] S. Hun Cheong, B. Y. Cho, J. Lee, C. Kim, and C. Nam, "Where to relocate?: Object rearrangement inside cluttered and confined environments for robotic manipulation," in *2020 IEEE International Conference on Robotics and Automation (ICRA)*, 2020, pp. 7791–7797.
- [21] H. Wang, W. Liang, and L.-F. Yu, "Scene mover: automatic move planning for scene arrangement by deep reinforcement learning," *ACM Trans. Graph.*, vol. 39, no. 6, pp. 1–15, dec 2020.
- [22] K. Mirakhor, S. Ghosh, D. Das, and B. Bhowmick, "Task planning for object rearrangement in multi-room environments," 2024.
- [23] H. Ren and A. H. Qureshi, "Multi-stage monte carlo tree search for non-monotone object rearrangement planning in narrow confined environments," in *2024 IEEE/RSJ International Conference on Intelligent Robots and Systems (IROS)*, 2024, pp. 12078–12085.
- [24] K. Gao, S. Feng, and J. Yu, "On minimizing the number of running buffers for tabletop rearrangement," in *Proceedings of Robotics: Science and Systems*, 2021.
- [25] K. Gao, Z. Ye, D. Zhang, B. Huang, and J. Yu, "Toward holistic planning and control optimization for dual-arm rearrangement," 2024.
- [26] H. Song, J. A. Hausteine, W. Yuan, K. Hang, M. Y. Wang, D. Kragic, and J. A. Stork, "Multi-object rearrangement with monte carlo tree search: A case study on planar nonprehensile sorting," in *2020 IEEE/RSJ International Conference on Intelligent Robots and Systems (IROS)*, 2020, pp. 9433–9440.
- [27] W. C. Agboh, S. Sharma, K. Srinivas, M. Parulekar, G. Datta, T. Qiu, J. Ichnowski, E. Solowjow, M. Dogar, and K. Goldberg, "Learning to efficiently plan robust frictional multi-object grasps," in *2023 IEEE/RSJ International Conference on Intelligent Robots and Systems (IROS)*, 2023, pp. 10660–10667.
- [28] K. Srinivas, S. Ganti, R. Parikh, A. Ahmad, W. Agboh, M. Dogar, and K. Goldberg, "The busboy problem: Efficient tableware decluttering using consolidation and multi-object grasps," in *2023 IEEE 19th International Conference on Automation Science and Engineering (CASE)*, 2023, pp. 1–6.
- [29] Z. Wu, J. Tang, X. Chen, C. Ma, X. Lan, and N. Zheng, "Prioritized planning for target-oriented manipulation via hierarchical stacking relationship prediction," in *2023 IEEE/RSJ International Conference on Intelligent Robots and Systems (IROS)*, 2023, pp. 4873–4880.
- [30] G. Jocher, "Ultralytics yolov5," 2020, software. [Online]. Available: <https://github.com/ultralytics/yolov5>
- [31] S. Ghasemi, H. Hosseini, M. Koosheshi, M. T. Masouleh, and A. Kalhor, "Scene understanding in pick-and-place tasks: Analyzing transformations between initial and final scenes," in *2024 32nd International Conference on Electrical Engineering (ICEE)*, 2024, pp. 1–7.
- [32] E. Coumans and Y. Bai, "Pybullet, a python module for physics simulation for games, robotics and machine learning," <http://pybullet.org>, 2016–2021.
- [33] P. E. Hart, N. J. Nilsson, and B. Raphael, "A formal basis for the heuristic determination of minimum cost paths," *IEEE Transactions on Systems Science and Cybernetics*, vol. 4, no. 2, pp. 100–107, 1968.
- [34] P. Viola and M. Jones, "Rapid object detection using a boosted cascade of simple features," in *Proceedings of the 2001 IEEE Computer Society Conference on Computer Vision and Pattern Recognition. CVPR 2001*, vol. 1, 2001.
- [35] C. Gaz, M. Cognetti, A. Oliva, P. Robuffo Giordano, and A. De Luca, "Dynamic identification of the franka emika panda robot with retrieval of feasible parameters using penalty-based optimization," *IEEE Robotics and Automation Letters*, vol. 4, no. 4, pp. 4147–4154, 2019.
- [36] A. H. Dastjerdi, M. M. Sheikhi, and M. T. Masouleh, "A complete analytical solution for the dimensional synthesis of 3-dof delta parallel robot for a prescribed workspace," *Mechanism and Machine Theory*, vol. 153, p. 103991, 2020.